inorganics

MDPI

Article

Reaction of Dialumane Incorporating Bulky Eind Groups with Pyridines

Takahiro Murosaki [1], Ryoma Ohno [1], Tomohiro Agou [2], Daisuke Hashizume [3] and Tsukasa Matsuo [1,*]

1 Department of Applied Chemistry, Faculty of Science and Engineering, Kindai University 3-4-1 Kowakae, Higashi-Osaka, Osaka 577-8502, Japan; takahiro.jtta@gmail.com (T.M.); 1833320221d@kindai.ac.jp (R.O.)
2 Department of Quantum Beam Science, Graduate School of Science and Engineering, Ibaraki University, 4-12-1 Naka-narusawa, Hitachi, Ibaraki 316-8511, Japan; tomohiro.agou.mountain@vc.ibaraki.ac.jp
3 RIKEN Center for Emergent Matter Science (CEMS), 2-1 Hirosawa, Wako, Saitama 351-0198, Japan; hashi@riken.jp
* Correspondence: t-matsuo@apch.kindai.ac.jp; Tel.: +81-6-4307-3462

Received: 30 September 2019; Accepted: 18 October 2019; Published: 25 October 2019

Abstract: The reaction of the bulky Eind-based dialumane, (Eind)HAl(μ-H)$_2$AlH(Eind) (**1**) (Eind = 1,1,3,3,5,5,7,7-octaethyl-*s*-hydrindacen-4-yl), with pyridines is described. When **1** was treated with pyridine (Py) in toluene, the Py adduct of aryldihydroalumane, Py→AlH$_2$(Eind) (**2**), was initially formed. Then, the hydroalumination of Py took place to yield the Py-bound aryl(1,4-dihydropyrid-1-yl)hydroalumane, Py→AlH(1,4-dihydropyrid-1-yl)(Eind) (**3**). A similar reaction with a stronger Lewis base, 4-pyrrolidinopyridine (PPy), produced the stable PPy adduct, PPy→AlH$_2$(Eind) (**4**). The resulting organoaluminum compounds have been fully characterized by NMR spectroscopy as well as X-ray crystallography. The reaction mechanism from **1** to **3** via **2** has been examined by deuterium labeling experiments using (Eind)DAl(μ-D)$_2$AlD(Eind) (**1-*d*$_4$**).

Keywords: organoaluminum compounds; aluminum hydrides; pyridines; hydroalumination; deuterium labeling reaction

1. Introduction

Aluminum hydrides have been widely used as a powerful reducing agent both in inorganic and organic synthesis, whose excellent reactivities are primarily based on polarized Al–H bonds due to the rather electropositive aluminum atom [1–8]. The aggregation behavior and structural characteristics of the hydrogen-substituted aluminum compounds both in solution and in the solid state have also been investigated for many years to understand their unique chemical bonding arising from the electron deficiency of the group 13 elements [1–8].

In contrast to the highly-reactive aluminum hydrides, a mixture of lithium aluminum hydride (LiAlH$_4$) and pyridine (Py), which is known as "Lansbury's reagent", shows a mild reactivity, thus being applied for the selective reduction of aldehydes and ketones in the presence of carboxylic acids and esters [9–11]. Tanner and Yang reported the detailed studies of the reaction between LiAlH$_4$ and Py; five isomers of lithium tetrakis(dihydropyridyl)aluminate having 1,2- or 1,4-dihydropyrid-1-yl ligands were observed during the initial stage, but gradually isomerized into a single final product with only the 1,4-dihydropyrid-1-yl ligand [12]. Then, Hensen et al. reported the crystal structures of lithium tetrakis(1,4-dihydropyrid-1-yl)aluminate and related aluminate compounds determined by an X-ray diffraction analysis [13]. They also examined the hydroalumination of Py using a neutral trihydroalumane-trimethylamine complex, Me$_3$N→AlH$_3$, yielding the Py-coordinated tris(1,4-dihydropyrid-1-yl)alumane [13]. These precedent studies clearly

indicated that the 1,4-dihydropyrid-1-yl group is thermally more stable than the 1,2-dihydropyrid-1-yl group on the aluminum center [14]. It is important to note that the dihydropyridine moiety ubiquitously exists in a biological redox system, the reduced form of nicotinamide adenine dinucleotide (NADH), involving electron transfer reactions [15].

We have recently synthesized some new discrete aluminum hydride compounds by introducing bulky aryl groups [16,17]. As shown in Scheme 1a, the aryldihydroalumane dimer [dialumane(6)], (Eind)HAl(μ-H)$_2$AlH(Eind) (**1**), incorporating the fused-ring bulky Eind groups (Eind = 1,1,3,3,5,5,7,7-octaethyl-*s*-hydrindacen-4-yl), was obtained by the treatment of the lithium aryltrihydroaluminate dimer, [Li(OEt$_2$)]$_2$[(Eind)AlH$_3$]$_2$ (**5**), with chlorotrimethylsilane (Me$_3$SiCl) [16]. Scheme 1b shows the facile activation of the dihydrogen (H$_2$) molecule by the barrelene-type of dialuminum compounds supported by the bulky aryl (Ar) groups [Ar = Tbb (**I**) and Bpb (**II**); Tbb = 2,6-{CH(SiMe$_3$)$_2$}$_2$-4-^{t}Bu-C$_6$H$_2$, Bpb = 2,6-{CH(SiMe$_3$)$_2$}$_2$-C$_6$H$_3$], thus also producing the corresponding dialuminum hydrides, (Ar)HAl(μ-H)$_2$AlH(Ar) [Ar = Tbb (**III**) and Bpb (**IV**)], concurrent with the release of benzene [17]. The molecular structures of the doubly hydrogen-bridged dimers of the aryldihydroalumanes **1** and **III** were determined by X-ray crystallography [16,17], and their dynamic monomer–dimer equilibriums in solution were examined by the crossover experiments, as shown in Scheme 1c, resulting in the formation of equilibrium mixtures containing asymmetrical dialumane, (Tbb)HAl(μ-H)$_2$AlH(Bpb) (**V**), and (Tbb)HAl(μ-H)$_2$AlH(Eind) (**VI**), as judged by the ^{1}H NMR spectra [17]. It is noteworthy that the dialuminum hydrides **V** and **VI** are rare examples of the group 13 element compounds containing asymmetrical three-center two-electron (3c-2e) bonds.

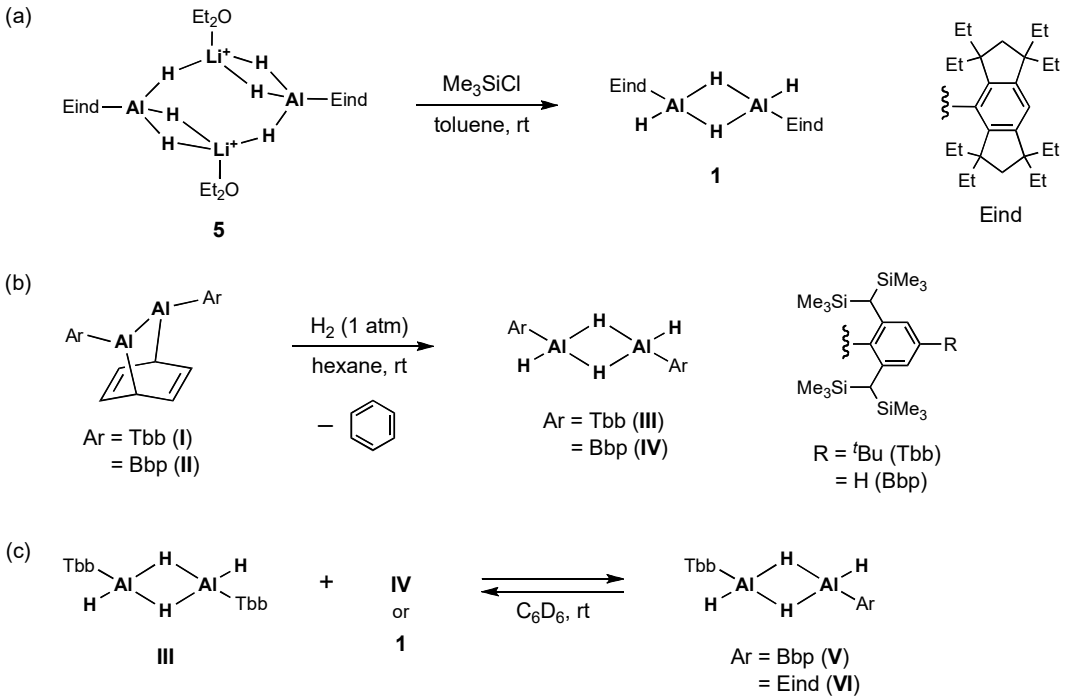

Scheme 1. (**a**) Synthesis of (Eind)HAl(μ-H)$_2$AlH(Eind) **1**, (**b**) Synthesis of (Ar)HAl(μ-H)$_2$AlH(Ar) [Ar = Tbb (**III**) and Bpb (**IV**)], and (**c**) Crossover reactions between **III** and **IV** or **1**.

In this article, we report the reactions of the bulky Eind-based dialumane **1** with pyridine (Py) and 4-pyrrolidinopyridine (PPy). The former reaction led to the formation of the Py-bound aryl(1,4-dihydropyrid-1-yl)hydroalumane, Py→AlH(1,4-dihydropyrid-1-yl)(Eind) (**3**), involving the hydroalumination reaction of Py with one of the two Al–H bonds in (Eind)AlH$_2$. The latter reaction afforded a simple PPy adduct, PPy→AlH$_2$(Eind) (**4**), in which the two Al–H bonds remained intact. The characterization of the resulting organoaluminum hydrides and a possible reaction mechanism between **1** and Py to form **3** are reported.

2. Results and Discussions

*2.1. Reaction of (Eind)HAl(μ-H)$_2$AlH(Eind) (**1**) with Pyridine (Py)*

As shown in Scheme 2, we first examined the reaction of **1** with the unsubstituted pyridine (Py). When four equivalents of Py were added to a suspension of **1** in toluene, the Py adduct of the aryldihydroalumane monomer, Py→AlH$_2$(Eind) (**2**), was initially formed, which could be characterized by NMR spectroscopy (Figures S1 and S2). The ^{1}H NMR spectrum of **2** in C_6D_6 shows a set of three resonances due to the coordinated Py molecule at δ = 8.20 (d, *J* = 5.0 Hz, 2 H, H-2,6), 6.56 (t, *J* = 7.8 Hz, 1 H, H-4), and 6.18 (dd, *J* = 7.8 and 5.0 Hz, 2 H, H-3,5) ppm. The *p*-aryl proton of the Eind group was observed at δ = 6.91 (s, 1 H, ArH) ppm. One broad signal at δ = 5.51 (br. s, 2 H, AlH) ppm is assignable to the Al–H bond, which is shifted to a lower field compared to those of **1** (δ = 5.10 and 4.84 ppm). In the ^{13}C NMR spectrum of **2**, a set of three signals for the coordinated Py also appeared at δ = 148.1 (C-2,6), 139.9 (C-4), and 124.7 (C-3,5) ppm. Unfortunately, we found that it was difficult to isolate **2** in a pure form due to its labile nature. Thus, the colorless solution of the reaction mixture mainly containing **2** and the remaining Py gradually changed to an orange color within 4 days. After the mixture was evaporated to dryness, the residual solid was recrystallized from hexane at −30 °C to afford the Py adduct of aryl(1,4-dihydropyrid-1-yl)hydroalumane, Py→AlH(1,4-dihydropyrid-1-yl)(Eind) (**3**), as orange crystals in 63% yield. During the course of the reaction, Py reacted with one of the two Al–H bonds in (Eind)AlH$_2$ to be converted into the 1,4-dihydropyrid-1-yl ligand.

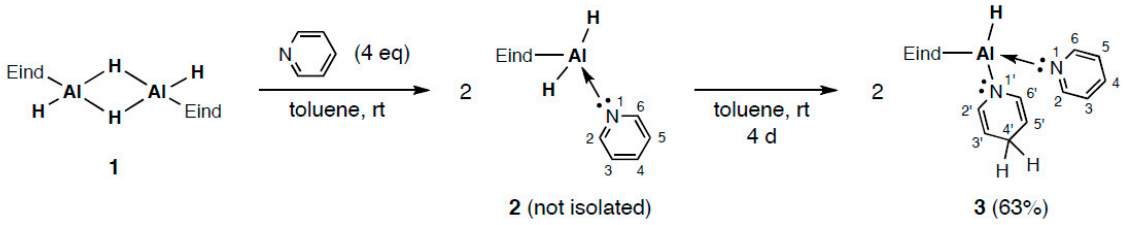

Scheme 2. Reaction of **1** with pyridine (Py).

Compound **3** has been characterized by NMR spectroscopy (Figures S3 and S4). In the ^{1}H NMR spectrum of **3** in C_6D_6, two sets of three signals due to the 1,4-dihydropyrid-1-yl ligand at δ = 6.13 (d, *J* = 8.3 Hz, 2 H, H-2′,6′), 4.53–4.56 (m, 2 H, H-3′,5′), and 3.42–3.44 (m, 2 H, H-4′) ppm, and the coordinated Py molecule at δ = 8.46 (br. d, 2 H, H-2,6), 6.64 (br. t, 1 H, H-4), and 6.34 (br. dd, 2 H, H-3,5) ppm were found, respectively, along with the *p*-aryl proton of the Eind group at δ = 6.87 (s, 1 H, ArH) ppm. The broad Al–H signal was observed at around δ = 5.25 (br. s, 1 H, AlH) ppm. The ^{13}C NMR spectrum of **3** exhibits a set of characteristic resonances for the 1,4-dihydropyrid-1-yl group at δ = 134.4 (C-2′,6′), 97.4 (C-3′,5′), and 24.3 (C-4′) ppm, together with the signals due to the coordinated Py at δ = 148.9 (C-2,6), 140.4 (C-4), and 124.9 (C-3,5) ppm. No detectable signal was observed in the solution ^{27}Al NMR spectrum of **3** despite a prolonged measurement. The UV–vis spectrum of **3** in benzene showed a weak absorption at 522 nm (ε = 750), which is responsible for the orange color of **3**.

*2.2. Reaction of (Eind)HAl(μ-H)$_2$AlH(Eind) (**1**) with 4-Pyrrolidinopyridine (PPy)*

We next investigated the reaction of **1** with a stronger Lewis base, 4-pyrrolidinopyridine (PPy), having an electron-donating pyrrolidino group at the 4-position of the Py ring (Scheme 3). By using PPy instead of Py, we have succeeded in the isolation of a Lewis base adduct of the monomeric aryldihydroalumane. After the addition of two equivalents of PPy to a suspension of **1** in toluene, the reaction mixture was stirred overnight at room temperature. The mixture was concentrated in vacuo and allowed to stand at −30 °C to afford colorless crystals of the PPy adduct of aryldihydroalumane, PPy→AlH$_2$(Eind) (**4**), in 50% yield. The PPy adduct **4** showed a rather good thermal stability in solution in comparison to the Py adduct, Py→AlH$_2$(Eind) **2**. Thus, while the Py adduct **2** slowly decomposed in C_6D_6 at room temperature even without an excess amount of Py, giving a mixture

containing **3** as a detectable product, the PPy adduct **4** was stable in C_6D_6 at room temperature under an argon atmosphere, even in the presence of an excess amount of PPy.

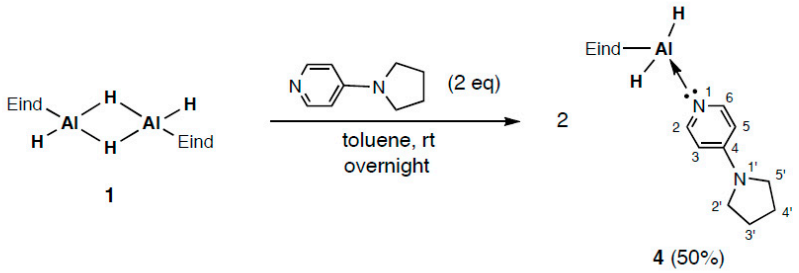

Scheme 3. Reaction of **1** with 4-pyrrolidinopyridine (PPy).

The formation of **4** was confirmed by NMR spectroscopic data (Figures S5 and S6). The ^{1}H NMR spectrum of **4** in C_6D_6 displays the signals due to the coordinated PPy at δ = 7.96 (d, *J* = 7.2 Hz, 2 H, H-2,6), 5.45 (d, *J* = 7.2 Hz, 2 H, H-3,5), 2.14–2.18 (m, 4 H, H-2′,5′), and 1.02–1.06 (m, 4 H, H-3′,4′) ppm. The *p*-aryl proton of the Eind group was observed at δ = 6.95 (s, 1 H, ArH) ppm. The Al–H signal of **4** was found at δ = 5.67 (br. s, 2 H, AlH) ppm, similar to that of **2** [δ = 5.51 (br. s, 2 H, AlH) ppm]. In the ^{13}C NMR spectrum of **4**, the resonances of the coordinated PPy appeared at δ = 152.5 (C-4), 147.5 (C-2,6), 106.9 (C-3,5), 46.5 (C-2′,5′), and 24.6 (C-3′,4′) ppm. The ^{27}Al NMR signal due to **4** could not be directly observed by ^{27}Al NMR spectroscopy.

*2.3. Structures of Py→AlH(1,4-dihydropyrid-1-yl)(Eind) (**3**) and PPy→AlH$_2$(Eind) (**4**)*

We have also examined the structures of **3** and **4** in the solid state. As shown in Figure 1, the molecular structure of **3** was determined by X-ray crystallography. In the crystals of **3**, the hydrogen atom (H1) on the aluminum atom (Al1) was located on the difference Fourier maps and isotropically refined. The mononuclear aluminum center has a distorted tetrahedral geometry with one hydrogen atom (H1), one carbon atom (C1) of the Eind group, and two nitrogen atoms (N1 and N2) of the 1,4-dihydropyrid-1-yl and Py ligands. The bond angles around the aluminum atom (C1–Al1–N1 = 112.75(8), C1–Al1–N2 = 117.05(8), and N1–Al1–N2 = 104.44(8)°) imply some steric hindrance between these coordinating ligands. The Al–C bond length in **3** (2.031(2) Å) is elongated compared to those in **1** (1.970(2) Å) [16] and **III** (1.957(4) Å) [17], which may be associated with the increasing electron density at the aluminum center due to the coordination of the 1,4-dihydropyrid-1-yl and Py ligands. The lengths of the two Al–N bonds in **3** are distinctly different from each other; thus, the Al–N distance for the 1,4-dihydropyrid-1-yl group (Al1–N1 = 1.8568(19) Å) is much shorter than that for the coordinated Py (Al1–N2 = 2.0050(19) Å), each of which corresponds to the covalent and dative Al–N bonds [13]. The N–C bond lengths in the 1,4-dihydropyrid-1-yl moiety (N1–C29 = 1.406(3) and N1–C33 = 1.394(3) Å) are longer than those in the coordinated Py ring (N2–C34 = 1.350(3) and N2–C38 = 1.350(3) Å). The differences in the C–C bond lengths are seen in the 1,4-dihydropyrid-1-yl skeleton: C29–C30 = 1.342(3), C30–C31 = 1.489(3), C31–C32 = 1.496(3), and C32–C33 = 1.344(3) Å. On the other hand, the coordinated Py ring has nearly the same C–C bond lengths: C34–C35 = 1.381(3), C35–C36 = 1.387(3), C36–C37 = 1.387(3), and C37–C38 = 1.377(3) Å. These structural characteristics found in **3** are analogous to those reported in the Py-adduct of tris(1,4-dihydropyrid-1-yl)alumane [13].

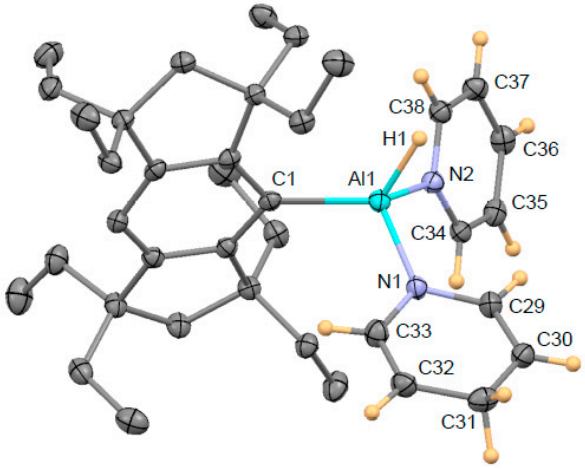

Figure 1. Molecular structure of **3**. The thermal ellipsoids are shown at the 50% probability level. The hydrogen atoms of the Eind group are omitted for clarity.

The X-ray diffraction analysis of **4** shows the presence of two crystallographically independent molecules of the mononuclear aluminum complex in the unit cell (molecules A and B). The hydrogen atoms on the aluminum atoms are located on the difference Fourier maps and isotropically refined. Since the two molecules are structurally similar, only the structure of molecule A is shown in Figure 2. The aluminum atom (Al1) is coordinated in a distorted tetrahedral manner by two hydrides (H1 and H2), one carbon atom (C1) of the Eind group, and one nitrogen atom (N1) of the PPy ligand. The C–Al–N bond angles in **4** (C1–Al1–N1 = 101.94(7)° for molecule A and C1B–Al1B–N1B = 106.72(8)° for molecule B) are much smaller than those in **3** (C1–Al1–N1 = 112.75(8) and C1–Al1–N2 = 117.06(8)°), which is probably due to the less steric hindrance at the aluminum atom. The dative Al–N bond length in **4** (Al1–N1 = 1.9842(17) Å) is somewhat shorter than that in **3** (Al1–N2 = 2.0049(19) Å), which is attributable to the stronger coordination ability of PPy relative to Py. However, the Al–C bond distance in **4** (Al1–C1 = 2.016(2) Å) is also slightly shorter than that in **3** (2.031(2) Å), even with the powerful coordination of PPy. These structural features may be ascribed to the delicate balance between the inherent properties of the hydride and 1,4-dihydropyrid-1-yl ligands and the steric congestion of the bulky Eind group and/or the crystal packing configuration, in addition to the coordination nature of the Py and PPy.

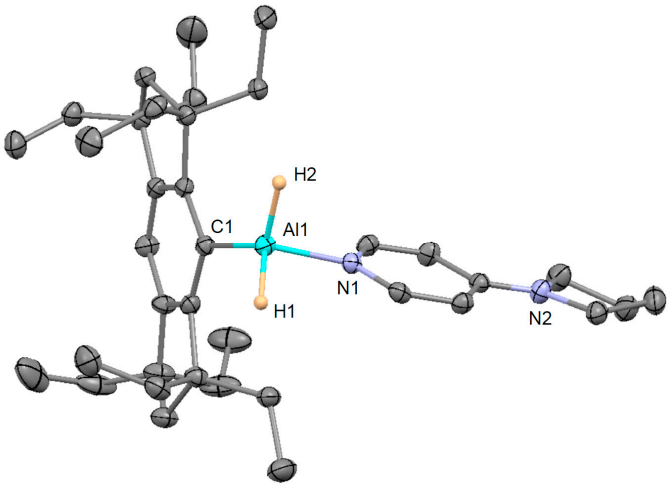

Figure 2. Molecular structure of **4** (molecule A). The thermal ellipsoids are shown at the 50% probability level. The hydrogen atoms, except for the Al–H groups, are omitted for clarity.

2.4. Mechanistic Studies on the Reaction from **1** to **3**

In order to obtain insight into the intervening processes during the reaction from **1** and Py to **3**, we performed deuterium labeling experiments employing the deuterated dialumane, (Eind)DAl(μ-D)$_2$AlD(Eind) (**1-*d*$_4$**), which was synthesized according to the reported procedure for **1** [16] (Scheme 4).

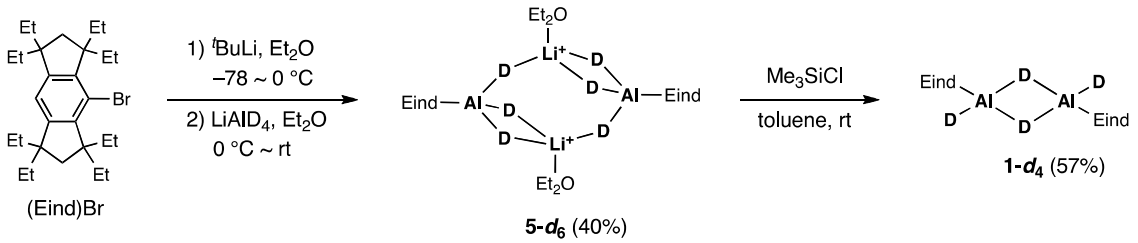

Scheme 4. Synthesis of **1-*d*$_4$**.

As shown in Scheme 4, the precursor, Eind-based lithium trideuterioaluminate dimer, [Li(OEt$_2$)]$_2$[(Eind)AlD$_3$]$_2$ (**5-*d*$_6$**), was synthesized by the addition of a suspension of lithium aluminum deuteride (LiAlD$_4$) in Et$_2$O to a solution of (Eind)Li, which was prepared by the treatment of (Eind)Br with two equivalents of ^{t}BuLi in Et$_2$O. After the reaction mixture was evaporated to dryness, benzene was added to the residue, and the resulting suspension was filtered to remove any insoluble materials. The filtrate was evaporated to dryness, and the resulting residual solid was washed with hexane to give **5-*d*$_6$** as a white solid in 40% yield. In the ^{2}H NMR spectrum of **5-*d*$_6$** in C$_6$H$_6$, one resonance due to the Al–D bond was observed at δ = 3.72 ppm (Figure S8), corresponding to the Al–H signal of **5** in the ^{1}H NMR spectrum in C$_6$D$_6$ (δ = 3.75 (br. s, 3 H, AlH) ppm) [16]. The ^{7}Li NMR spectrum of **5-*d*$_6$** displayed one signal appearing at δ = 2.57 ppm (Figure S9), similar to that of **5** (δ = 2.55 ppm) [16]. In the ^{27}Al NMR spectrum of **5-*d*$_6$**, a very broad signal was found at δ = 39.2 ($W_{1/2}$ = 8200 Hz) ppm (Figure S10), comparable to that found in **5** (δ = 48.3 ppm, $W_{1/2}$ = 7100 Hz) [16].

The deuterated dialumane **1-*d*$_4$** was prepared by the treatment of **5-*d*$_6$** with an excess amount (10 equivalents) of Me$_3$SiCl in toluene [16]. The reaction mixture was evaporated to dryness; then, toluene was re-added to the residue extracted by gently heating. After the removal of any insoluble materials by filtration, the filtrate was concentrated to dryness, and the resulting solid was washed with hexane to afford **1-*d*$_4$** as a white solid in 57% yield. The ^{2}H NMR spectrum of **1-*d*$_4$** in C$_6$H$_6$ exhibited two resonances at δ = 5.09 and 4.87 ppm assignable to the Al–D groups (Figure 3a and Figure S13), which are analogous to the Al–H signals in the ^{1}H NMR spectrum of **1** in C$_6$D$_6$ (δ = 5.10 (br. s, 2 H, AlH) and 4.84 (br. s, 2 H, AlH) ppm) [16]. The ^{27}Al NMR spectrum of **1-*d*$_4$** showed a very broad signal at δ = 52.3 ($W_{1/2}$ = 6100 Hz) ppm (Figure S14), similar to that of **1** (δ = 71.2 ppm, $W_{1/2}$ = 5300 Hz) [16].

We examined the NMR tube scale reaction of **1-*d*$_4$** with four equivalents of Py in C$_6$H$_6$ at room temperature. Figure 3 shows the progress of the reaction monitored by ^{2}H NMR spectroscopy (Figures S15–S18). We found that the reaction of the deuterated **1-*d*$_4$** with Py proceeds more slowly compared to the reaction of the non-deuterated **1** with Py, presumably due to the kinetic isotope effects involving the activation of the Al–H(D) and C–H(D) bonds during the rate-determining steps.

As shown in Figure 3a,b, the two resonances at δ = 5.09 and 4.87 ppm due to the Al–D groups of **1-*d*$_4$** disappeared in the ^{2}H NMR spectrum of the reaction mixture after 22 h. Thus, the dialumane **1-*d*$_4$** was fully consumed by the addition of Py within 1 day, giving Py→AlD$_2$(Eind) (**2-*d*$_2$**) as the initial product (Scheme 5). The main signal was observed at δ = 5.52 ppm, together with a small signal at δ = 8.37 ppm. The former signal corresponds to the Al–H signal of **2** in the ^{1}H NMR spectrum in C$_6$D$_6$ (δ = 5.51 (br. s, 2 H, AlH)). The latter signal may be due to the deuterium atom attached to the C–2,6 carbons of the coordinated Py ring in an isomer of **2-*d*$_2$** such as **B** (Scheme 5). Therefore, a facile H/D exchange took place between the Al–D bonds and the C–H bonds only at the 2,6-positions of the coordinated Py in **2-*d*$_2$**, most likely through the deuterioalumination of

the coordinated Py to form aryl(1-hydro-2-deuteriopyrid-1-yl)deuterioalumane (**A**) as a reaction intermediate. In this step from **2-d_2** to **A**, one of the possible processes is the reaction between the Al–D and N=C bonds in the four-membered ring transition state (**TS**), leading to the formation of the Al–N and C–D bonds to produce **A**. The deuterioalumination product **A** has a thermally unstable 1-hydro-2-deuteriopyrid-1-yl ligand [12,13], which may tend to convert to the aromatic Py ligand. While the migration of the deuterium atom from the 1-hydro-2-deuteriopyrid-1-yl ligand to the aluminum center can reproduce **2-d_2** with the non-deuterated Py ligand, the migration of the hydrogen atom may predominantly occur due to the kinetic isotope effect, giving **B** with the 2-deuteriopyridine ligand. A further deuterioalumination reaction of the coordinated 2-deuteriopyridine may produce **C** with the 1-hydro-2,6-dideuteriopyrid-1-yl ligand, and the subsequent hydrogen migration may afford **D** with the 2,6-dideuteriopyridine ligand.

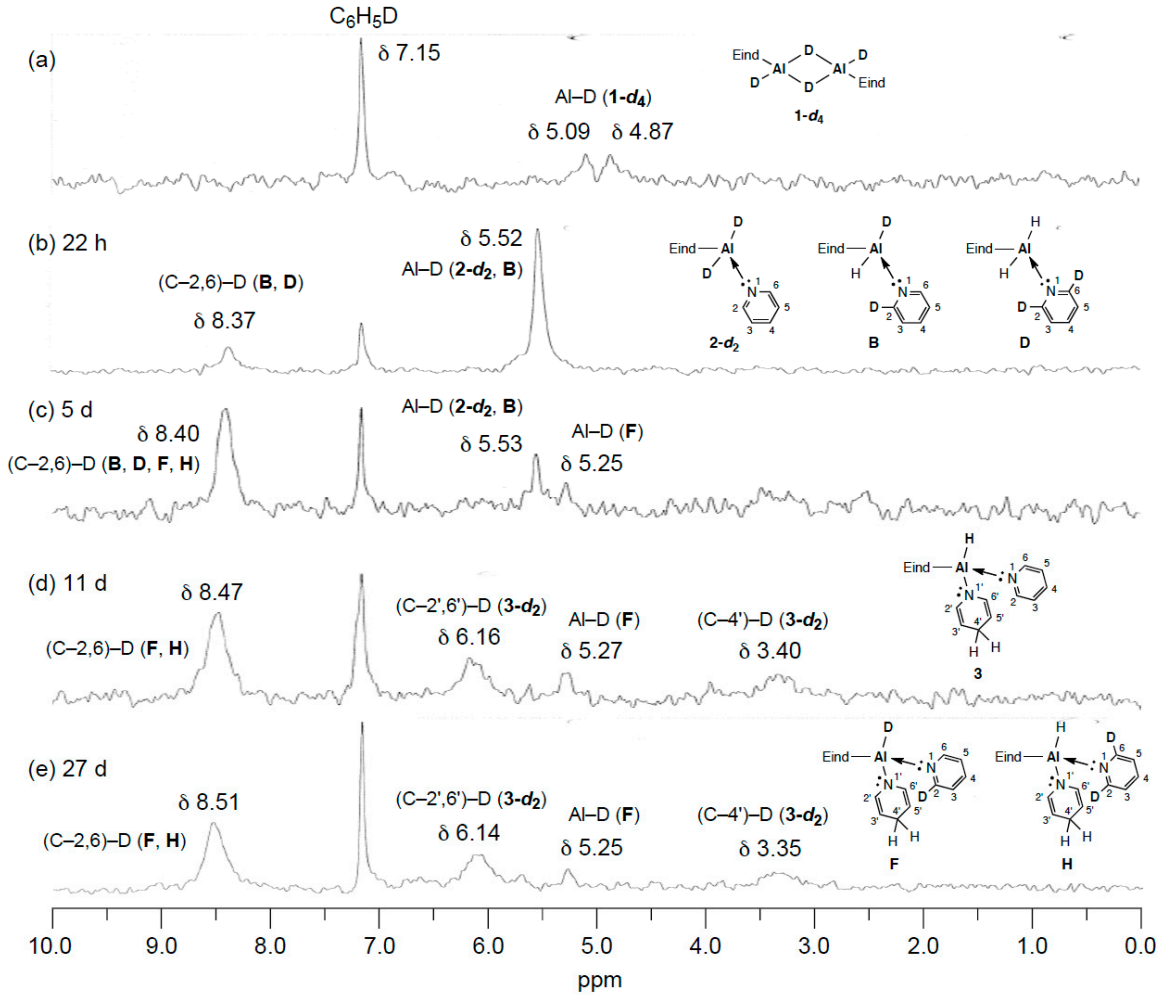

Figure 3. (**a**) ^{2}H NMR spectrum of **1-d_4** in C_6H_6 at room temperature, and ^{2}H NMR spectra of the reaction mixture of **1-d_4** and Py in C_6H_6 at room temperature; (**b**) after 22 h, (**c**) after 5 days, (**d**) after 11 days, and (**e**) after 27 days.

The reaction gradually proceeded at room temperature, during which time the intensity of the lower field signal increased (δ = 8.40 ppm), while the intensity of the higher field signal decreased (δ = 5.53 ppm), as shown in Figure 3c. A small signal was also found at δ = 5.25 ppm, which corresponds to the Al–H signal of **3** in the ^{1}H NMR spectrum in C_6D_6 (δ = 5.25 (br. s, 1 H, AlH) ppm), thus indicating the formation of a deuterated compound of **3** with the Al–D bond such as **F** (Scheme 5). Interestingly, although some very weak broad resonances appeared in the higher field region (δ = 2.0–4.0 ppm), almost no clear signal due to the deuteration of the 1,4-dihydropyrid-1-yl ligand was observed in the

^{2}H NMR spectra for at least 5 days. This indicated that after an additional Py molecule is coordinated to the electron-deficient aluminum center in **A** to form **E** (the Py adduct of **A**), the migration of the hydrogen atom rather than the deuterium atom from the 1-hydro-2-deuteriopyrid-1-yl ligand to the coordinated Py takes place in **E** by the kinetic isotope effect, leading to the formation of a thermally stable product **F** having the non-deuterated 1,4-dihydropyrid-1-yl and 2-deuteriopyridine ligands. Although the precise mechanism of the transformation of **E** into **F** is not clear at this moment, one of the possible resonance structures with a zwitterionic form (**E′**) may be responsible for the migration of the hydrogen atom. Density functional theory (DFT) calculations (B3LYP-D3/6-31G(d,p) level) indicate that the isomer of **3** having the 1,2-dihydropyrid-1-yl ligand (like **E**) is found at the 3.725 kcal mol^{-1} higher energy level. Similarly, the coordination of Py to **C** may afford **G** (the Py adduct of **C**); then, the hydrogen migration may produce a thermally stable product **H** with the 1,4-dihydropyrid-1-yl and 2,6-dideuteriopyridine ligands.

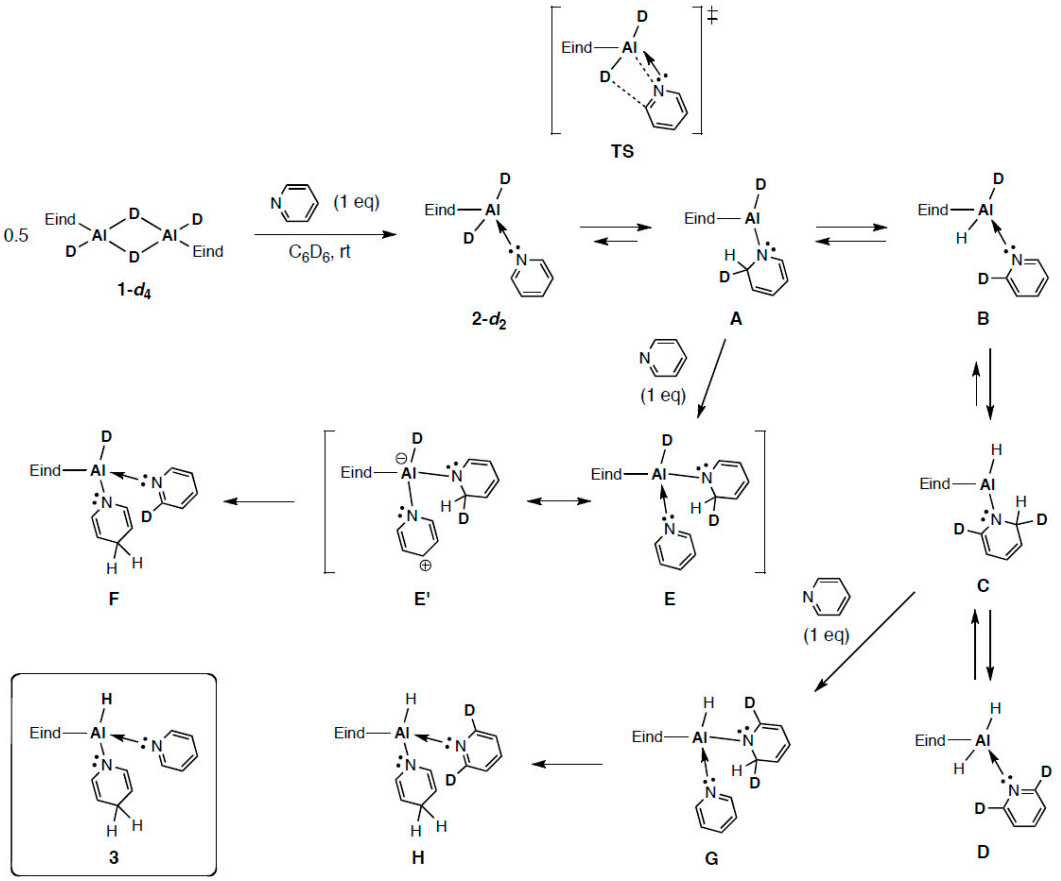

Scheme 5. Possible reaction mechanism between **1-*d*$_4$** and Py.

In the ^{2}H NMR spectrum of the reaction mixture after 11 days (Figure 3d), the main signal was observed at δ = 8.47 ppm, which is assignable to the deuterium atom(s) attached to the C-2,6 carbons of the coordinated Py ring in adducts **F** and **H**. The resonance at δ = 5.53 ppm disappeared in the ^{2}H NMR spectrum, indicating that **2-*d*$_2$** and its isomers were consumed during the reaction. The signals appearing at δ = 6.16 and 3.40 ppm may be due to the deuterium atoms attached to the C-2′,6′ and C-4′ carbons of the 1,4-dihydropyrid-1-yl ligand, each of which is corresponding to the C–H signals of **3** in the ^{1}H NMR spectrum in C_6D_6 (δ = 6.13 (d, *J* = 8.3 Hz, 2 H, H–2′,6′) and 3.42–3.44 (m, 2 H, H–4′) ppm). The observed relatively slow deuteration of the 1,4-dihydropyrid-1-yl ligand may result from the migration of the deuterium atom, the ligand exchange reaction between the deuterated and non-deuterated pyridines, etc. The ^{2}H NMR spectrum of the reaction mixture after 27 days (Figure 3e)

is very similar to that after 11 days (Figure 3d), indicating that the reaction was completed within a few weeks to cleanly produce the deuterated compounds of **3** (**3-d_2**), including **F** and **H**.

*2.5. Theoretical Calculations of **3***

To investigate the chemical bonding and electronic properties of **3**, we carried out DFT calculations at the B3LYP-D3/6-31G(d,p) level using the Gaussian 09 program package. The optimized structure well reproduces the experimental X-ray structure, having both the covalent and dative Al–N bonds (Al1–N1 = 1.863 and Al1–N2 = 2.084 Å). The calculated Al–C bond length in **3** (Al1–C1 = 2.014 Å) is longer than that in **1** (1.974 Å), being in good agreement with the experimental results. The bond lengths in the 1,4-dihydropyrid-1-yl moiety were also calculated to be similar to those found in the crystal structure (N1–C29 = 1.401, N1–C33 = 1.403, C29–C30 = 1.344, C30–C31 = 1.512, C31–C32 = 1.513, and C32–C33 = 1.342 Å).

The bond orders based on the Wiberg bond index (WBI) may provide insight into the chemical bonding in **3**. Interestingly, the terminal Al1–H1 bond order (0.729) is higher than the Al1–C1 bond order (0.562), which is probably due to the more polarized Al–C bond compared to the Al–H bond based on the electronegativities of the associated atoms: H 2.20, C 2.50, N 3.07, and Al 1.47 [18]. Similar WBI values are also computed for the terminal Al–H (0.820) and Al–C (0.620) bonds in **1**. However, during the reaction between **1** and Py, we could not experimentally observe any reactivity of the Al–C bond, which was probably due to the excellent steric protection of the bulky Eind group. We have also found that the covalent Al1–N1 bond order (0.369) for the 1,4-dihydropyrid-1-yl group is higher than the dative Al1–N2 bond order (0.226) for the coordinated Py molecule.

The natural population analysis (NPA) charge distribution of **3** also shows that the Al1–C1 bond is more highly polarized than the Al1–H1 bond with Al1(+1.623), C1(−0.567), and H1(−0.445), being similar to those values calculated for **1** with Al(+1.248), C(−0.557), and terminal-H(−0.347). The covalent Al1–N1 bond is more polarized than the dative Al1–N2 bond with the larger negative N1(−0.912) relative to N2(−0.591).

Figure 4 depicts the selected molecular orbitals (MOs) of **3** and their energy levels. While the highest occupied MO (HOMO) consists of the 1,4-dihydropyrid-1-yl unit, the lowest unoccupied MO (LUMO) and LUMO+1 are represented by the two π*(Py) orbitals. The absorption wavelength is computed to be 580 nm based on the TD-DFT calculations, comparable to the observed value (522 nm), which is mainly assignable to the intramolecular charge transfer (ICT) transition from the HOMO to the LUMO+1.

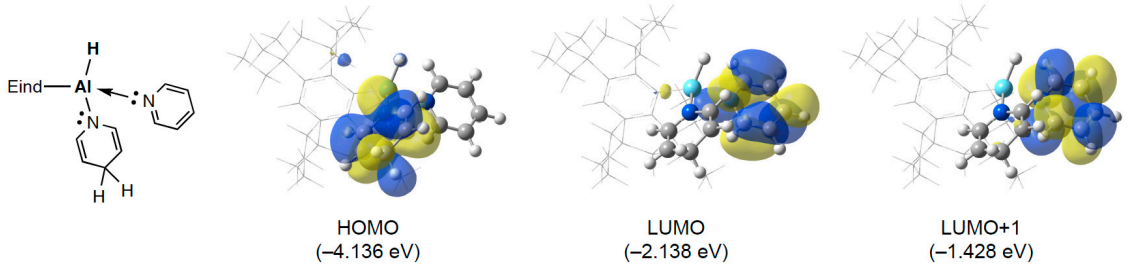

Figure 4. Selected molecular orbitals of **3** together with the energy levels.

3. Materials and Methods

3.1. General Procedures

All experimental manipulations of the air-sensitive and/or moisture-sensitive organometallic compounds were carried out either using standard Schlenk-line techniques or in a glove box filled with argon gas. All dried solvents, hexane, benzene, toluene, and diethyl ether (Et_2O) were purified with the GlassContour solvent dispensing system (Nikko Hansen and Co., Ltd., Osaka, Japan). Deuterated benzene (benzene-d_6, C_6D_6) was dried over a potassium mirror and vacuum

transferred prior to use. Pyridine (Py) was dried and distilled over calcium hydride (CaH_2) prior to use. 4-Bromo-1,1,3,3,5,5,7,7-octaethyl-*s*-hydrindacene, (Eind)Br, and the Eind-substituted dialumane, (Eind)HAl(μ-H)$_2$AlH(Eind) (**1**), were prepared by the literature methods [16,19]. All other chemicals and gases were used as received.

Nuclear magnetic resonance (NMR) spectra were recorded on a JEOL ECS-400 spectrometer (JEOL Ltd., Tokyo, Japan) (399.8 MHz for ^{1}H, 61.4 MHz for ^{2}H, 155.4 MHz for ^{7}Li, 100.5 MHz for ^{13}C, and 104.2 MHz for ^{27}Al) at room temperature (20 °C). Chemical shifts (δ) are expressed in parts per million (ppm) using the residual solvent peak for ^{1}H (residual C_6D_5H in C_6D_6, ^{1}H(δ) = 7.15), ^{2}H (C_6H_5D: ^{2}H(δ) = 7.15), and for ^{13}C (C_6D_6: ^{13}C(δ) = 128.0) with coupling constants in Hertz (Hz). NMR multiplicities are abbreviated as singlet (s), doublet (d), triplet (t), quartet (q), multiplet (m), and broad (br). The UV–vis absorption spectra were recorded on a Shimadzu UV-3101(PC)S spectrometer (Shimadzu corporation, Kyoto, Japan). The elemental analyses were carried out by the Materials Characterization Support Team of the RIKEN Center for Emergent Matter Science (CEMS) (Wako, Japan). Melting points (mp) were recorded on a Stanford Research Systems (SRS) OptiMelt instrument (SRS, Sunnyvale, CA, USA). Due to extremely high air and moisture sensitivity, satisfactory results of the elemental analyses for **3** and **4** could not be obtained. Their purities were confirmed by the NMR spectra, as shown in Figures S3–S6.

3.1.1. Synthesis of Py→AlH(1,4-dihydropyrid-1-yl)(Eind) (**3**)

To a suspension of **1** (299 mg, 0.364 mmol) in toluene (7 mL), pyridine (120 μL, 118 mg, 1.49 mmol) was added at room temperature. After 2 h, the formation of Py→AlH_2(Eind) (**2**) was measured by NMR spectroscopy (Figures S1 and S2). The reaction mixture was stirred at room temperature for 4 days, during which time the solution color changed from colorless to orange. Then, the mixture was concentrated in vacuo. The residue was recrystallized from hexane at −30 °C to give **3** as orange crystals in 63% yield (261 mg, 0.459 mmol).

2: ^{1}H NMR (399.8 MHz, C_6D_6, 20 °C): δ = 0.88 (t, *J* = 7.3 Hz, 12 H, CH_2CH_3), 0.99 (t, *J* = 7.3 Hz, 12 H, CH_2CH_3), 1.71–1.85 (m, 8 H, CH_2CH_3), 1.90 (s, 4 H, CH_2), 2.16–2.25 (m, 4 H, CH_2CH_3), 2.38–2.48 (m, 4 H, CH_2CH_3), 5.51 (br. s, 2 H, AlH), 6.18 (dd, *J* = 7.8 and 5.0 Hz, 2 H, H-3,5), 6.56 (t, *J* = 7.8 Hz, 1 H, H-4), 6.91 (s, 1 H, ArH), 8.20 (d, *J* = 5.0 Hz, 2 H, H-2,6); ^{13}C NMR (100.5 MHz, C_6D_6, 20 °C): δ = 9.6, 10.2, 34.0, 34.1, 43.5, 47.8, 53.7, 119.9, 124.7 (C-3,5), 139.9 (C-4), 147.5, 148.1 (C-2,6), 158.8 (one peak of the aromatic carbon, ipso position to the aluminum, was not observed).

3: ^{1}H NMR (399.8 MHz, C_6D_6, 20 °C): δ = 0.89 (t, *J* = 7.4 Hz, 12 H, CH_2CH_3), 0.95 (t, *J* = 7.3 Hz, 12 H, CH_2CH_3), 1.64–1.82 (m, 8 H, CH_2CH_3), 1.86 (s, 4 H, CH_2), 1.90–2.30 (br. m, 8 H, CH_2CH_3), 3.42–3.44 (m, 2 H, H-4′), 4.53–4.56 (m, 2 H, H-3′,5′), 5.25 (br. s, 1 H, AlH), 6.13 (d, *J* = 8.3 Hz, 2 H, H-2′,6′), 6.34 (br. dd, 2 H, H-3,5), 6.64 (br. t, 1 H, H-4), 6.87 (s, 1 H, ArH), 8.46 (br. d, 2 H, H-2,6); ^{13}C NMR (100.5 MHz, C_6D_6, 20 °C): δ = 9.6, 10.3, 24.3 (C-4′), 34.2 (×2), 43.4, 47.9, 53.1, 97.4 (C-3′,5′), 119.9, 124.9 (C-3,5), 134.4 (C-2′,6′), 140.4 (C-4), 147.7, 148.9 (C-2,6), 158.8 (one peak of the aromatic carbon, ipso position to the aluminum, was not observed). Anal. Calcd. for $C_{38}H_{57}AlN_2$: C, 80.23; H, 10.10; N, 4.92. Found: C, 78.39; H, 9.94; N, 5.07. Melting point (argon atmosphere in a sealed tube) 135–141 °C (dec.).

3.1.2. Synthesis of PPy→AlH_2(Eind) (**4**)

To a suspension of **1** (201 mg, 0.245 mmol) in toluene (3 mL), 4-pyrrolidino-pyridine (PPy) (73.1 mg, 0.493 mmol) was added at room temperature. The reaction mixture was stirred overnight at room temperature. Then, the mixture was concentrated in vacuo and allowed to stand at −30 °C to give **4** as colorless crystals in 50% yield (136 mg, 0.243 mmol).

4: ^{1}H NMR (399.8 MHz, C_6D_6, 20 °C): δ = 0.99–1.06 (m, 28 H, CH_2CH_3 and H-3′,4′), 1.76–1.92 (m, 8 H, CH_2CH_3), 1.98 (s, 4 H, CH_2), 2.14–2.18 (m, 4 H, H-2′,5′), 2.35–2.44 (m, 4 H, CH_2CH_3), 2.61–2.69 (m, 4 H, CH_2CH_3), 5.45 (d, *J* = 7.2 Hz, 2 H, H-3,5), 5.67 (br. s, 2 H, AlH), 6.95 (s, 1 H, ArH), δ = 7.96 (d, *J* = 7.2 Hz, 2 H, H-2,6); ^{13}C NMR (100.5 MHz, C_6D_6, 20 °C): δ = 9.7, 10.4, 24.6 (C-3′,4′), 34.1, 34.1(×2), 43.6, 46.5 (C-2′,5′), 47.8, 53.8, 106.9 (C-3,5), 119.3, 147.2, 147.5 (C-2,6), 152.5 (C-4), 158.7 (one peak of the

aromatic carbon, ipso position to the aluminum, was not observed). Anal. Calcd. for $C_{38}H_{57}AlN_2$: C, 79.52; H, 10.64; N, 5.01. Found: C, 78.62; H, 10.56; N, 4.99. Melting point (argon atmosphere in a sealed tube) 194–196 °C (dec.).

3.1.3. Synthesis of $[Li(OEt_2)]_2[(Eind)AlD_3]_2$ (**5-*d*$_6$**)

^{t}BuLi (1.61 M in pentane, 2.70 mL, 4.35 mmol) was slowly added to a solution of (Eind)Br (927 mg, 2.01 mmol) in Et_2O (60 mL) at −78 °C. The mixture was allowed to warm to 0 °C with stirring. A suspension of $LiAlD_4$ (127 mg, 3.03 mmol) in Et_2O (15 mL) was added to the resulting solution of (Eind)Li at 0 °C. After the mixture was stirred for 5 h at room temperature, the volatiles were removed in vacuo to yield a gray solid. Benzene (60 mL) was added to the residue, and the resulting suspension was filtered through Celite (Wako Pure Chemicals Industries, Ltd., Osaka, Japan). The filtrate was concentrated in vacuo to afford a white solid, which was washed with hexane to give **5-*d*$_6$** as a white solid in 40% yield (400 mg, 0.403 mmol).

5-*d*$_6$: ^{1}H NMR (399.8 MHz, C_6D_6, 20 °C): δ = 0.96 (t, *J* = 7.4 Hz, 24 H, CH_2CH_3), 1.03 (t, *J* = 7.3 Hz, 24 H, CH_2CH_3), 1.03 (t, *J* = 7.3 Hz, 12 H, Et_2O), 1.66–1.83 (m, 16 H, CH_2CH_3), 1.92 (s, 8 H, CH_2), 2.21–2.28 (m, 16 H, CH_2CH_3), 3.16 (br. q, 8 H, Et_2O), 6.86 (s, 2 H, ArH); ^{2}H NMR (61.4 MHz, C_6H_6, 20 °C): δ = 3.72; ^{7}Li NMR (155.4 MHz, C_6D_6, 20 °C): δ = 2.57; ^{27}Al (104.2 MHz, C_6D_6, 20 °C): δ = 39.2 ($W_{1/2}$ = 8200 Hz).

3.1.4. Synthesis of (Eind)DAl(μ-D)$_2$AlD(Eind) (**1-*d*$_4$**)

To a solution of **5-*d*$_6$** (251 mg, 0.253 mmol) in toluene (30 mL), Me_3SiCl (320 μL, 274 mg, 2.52 mmol) was added at room temperature, and the solution was stirred for 1 h, and then evaporated to dryness. To the residue, toluene (30 mL) was added. The resulting suspension was gently heated using a hairdryer and filtered through a glass filter. The filtrate was concentrated in vacuo, and the remaining white solid was washed with hexane to give **1-*d*$_4$** as a white solid in 57% yield (120 mg, 0.145 mmol).

1-*d*$_4$: ^{1}H NMR (399.8 MHz, C_6D_6, 20 °C): δ = 0.92 (t, *J* = 7.3 Hz, 24 H, CH_2CH_3), 0.99 (t, *J* = 7.3 Hz, 24 H, CH_2CH_3), 1.60–1.75 (m, 16 H, CH_2CH_3), 1.83 (s, 8 H, CH_2), 1.93–2.02 (m, 8 H, CH_2CH_3), 2.10–2.20 (m, 8 H, CH_2CH_3), 6.92 (s, 2 H, ArH); ^{2}H NMR (61.4 MHz, C_6H_6, 20 °C): δ = 4.87, 5.09; ^{13}C NMR (100.5 MHz, C_6D_6, 20 °C): δ = 9.5, 9.8, 33.5, 34.8, 41.6 48.4, 52.4, 121.6, 147.5, 158.5 (one peak of the aromatic carbon, ipso position to the aluminum, was not observed). ^{27}Al (104.2 MHz, C_6D_6, 20 °C): δ = 52.3 ($W_{1/2}$ = 6100 Hz).

3.1.5. Reaction of (Eind)DAl(μ-D)$_2$AlD(Eind) (**1-*d*$_4$**) with Py

To a solution of **1-*d*$_4$** (9.9 mg, 12.0 μmol) in benzene (0.5 mL), pyridine (3.90 μL, 3.83 mg, 48.4 mmol) was added at room temperature. The progress of the reaction was monitored by ^{2}H NMR spectroscopy. The ^{2}H NMR spectra were observed after 22 h (Figure S15), 5 days (Figure S16), 11 days (Figure S17), and 27 days (Figure S18), as shown in Figure 3.

3.2. X-ray Crystallographic Studies of **3** *and* **4**

X-ray quality single crystals were obtained from saturated solutions of **3** in hexane and **4** in toluene. Intensity data were collected on a Rigaku XtaLAB P200 with a PILATUS200 K detector for **3** and a Rigaku AFC-10 with Saturn 724 CCD detector for **4**. Measurements were performed using Mo Kα radiation (λ = 0.71073 Å) (Rigaku corporation, Tokyo, Japan). The programs of CrysAlisPro [20] for **3** and CrystalClear [21] were used for the integration and scaling of the diffraction data, after the Lorentz, polarization, and the absorption corrections. The structures were solved by an iterative method with the program of SIR2011 [22] for **3** and SIR2004 [23] for **4**, and refined by a full-matrix least-squares method on F^2 for all the reflections using the SHELXL-2018/3 program [24]. All of the non-hydrogen atoms were refined anisotropically. Fourier maps showed the positions of all the hydrogen atoms. The hydrogen atoms of the Al–H moieties were isotropically refined, and the other H atoms were refined as riding models. CIF files can be obtained from the Cambridge Crystal Data Centre (CCDC numbers 1956662

and 1956663) via http://www.ccdc.cam.ac.uk/conts/retrieving.html (or from the CCDC, 12 Union Road, Cambridge CB2 1EZ, UK; Fax: +44-1223-336033; E-mail: deposit@ccdc.cam.ac.uk).

3.2.1. Py→AlH(1,4-dihydropyrid-1-yl)(Eind) (**3**)

$C_{38}H_{57}AlN_2$, M = 568.83, crystal size 0.25 × 0.21 × 0.16 mm, monoclinic, space group $P2_1/c$ (#14), a = 15.694(3) Å, b = 12.3466(19) Å, c = 18.341(3) Å, β = 110.986(3)°, V = 3318.2(10) Å^3, Z = 4, D_x = 1.139 g cm^{-3}, μ(Mo Kα) = 0.089 mm^{-1}, 53,312 reflections collected, 7584 unique reflections, and 382 refined parameters. The final $R(F)$ value was 0.0695 [$I > 2\sigma(I)$]. The final $R_w(F^2)$ value was 0.1599 (all data). The goodness-of-fit on F^2 was 1.153.

3.2.2. PPy→AlH_2(Eind) (**4**)

$C_{37}H_{59}AlN_2$, M = 558.84, crystal size 0.20 × 0.14 × 0.13 mm, triclinic, space group $P1-$ (#2), a = 11.526(2) Å, b = 16.394(3) Å, c = 18.301(4) Å, α = 86.889(5)°, β = 85.498(6)°, γ = 81.568(5)°, V = 3406.8(11) Å^3, Z = 4, D_x = 1.090 g cm^{-3}, μ(Mo Kα) = 0.086 mm^{-1}, 56,627 reflections collected, 15,570 unique reflections, and 753 refined parameters. The final $R(F)$ value was 0.0675 [$I > 2\sigma(I)$]. The final $R_w(F^2)$ value was 0.1528 (all data). The goodness-of-fit on F^2 was 1.091.

4. Conclusions

We have investigated the reactions of the fused-ring bulky Eind-substituted dialumane, (Eind)HAl(μ-H)$_2$AlH(Eind) (**1**), with pyridine (Py) and 4-pyrrolidinopyridine (PPy). While **1** reacted with Py to produce the Py-coordinated aryl(1,4-dihydropyrid-1-yl)hydroalumane, Py→AlH(1,4-dihydropyrid-1-yl)(Eind) (**3**), through the formation of the Py adduct of aryldihydroalumane, Py→AlH_2(Eind) (**2**), as the intermediate, the reaction with PPy resulted in the isolation of the PPy adduct of aryldihydroalumane, PPy→AlH_2(Eind) (**4**). We have also examined the formation mechanism of **3** in association with the hydroalumination of Py by the deuterium labeling experiments using (Eind)DAl(μ-D)$_2$AlD(Eind) (**1-*d*$_4$**). These reactions are mainly dependent on the basicity of the pyridines and the polarized Al–H bonds under the influence of the steric effects of the bulky substituent at the aluminum atom. Further studies of the reactivities of **1** and related compounds of the Group 13 elements are now in progress.

Supplementary Materials: The following are available online at http://www.mdpi.com/2304-6740/7/11/129/s1, NMR spectra of **2**, **3**, **4**, **5-*d*$_6$**, and **1-*d*$_4$** (PDF), crystallographic details for **3** and **4** (CIF), and CIF-checked files (PDF).

Author Contributions: T.M. (Takahiro Murosaki) performed the experiments. R.O. and D.H. carried out the X-ray crystallographic analysis. T.A and T.M. (Tsukasa Matsuo) designed the experiments. T.M. (Tsukasa Matsuo) directed the project and wrote the paper. T.A. and D.H. reviewed and approved the final manuscript. All authors contributed to the discussions.

Funding: This study was supported by Grants-in-Aid for Scientific Research on Innovative Areas "Coordination Asymmetry: Design and Asymmetric Coordination Sphere and Anisotropic Assembly for the Creation of Functional Molecules (No. 2802)" (JSPS KAKENHI Grant Nos. JP19H04601 for T. Matsuo) and Scientific Research (C) (No. JP18K05160 for T. Matsuo). We thank the Collaborative Research Program of Institute for Chemical Research, Kyoto University (grants #2018-110 and #2019-120).

Acknowledgments: We thank K. Nagata, T. Sasamori, and N. Tokitoh for their valuable discussions. We are grateful to the Materials Characterization Support Team, RIKEN Center for Emergent Matter Science (CEMS), for the elemental analyses.

Conflicts of Interest: The authors declare no conflict of interest.

References

1. Cowley, A.H.; Gabbaï, F.P.; Isom, H.S.; Dechen, A. New developments in the organoaluminum and organogallium hydrides. *J. Organomet. Chem.* **1995**, *500*, 81–88. [CrossRef]
2. Seyden-Penna, J. *Reductions by the Alumino and Borohydrides in Organic Synthesis*, 2nd ed.; Wiley-VCH: Weinheim, Germany, 1997.

3. Downs, A.J. Recent advances in the chemistry of Group 13 metals: Hydride derivatives and compounds involving multiply bonded Group 13 metal atom. *Coord. Chem. Rev.* **1999**, *189*, 59–100. [CrossRef]
4. Wehmschulte, R.J.; Power, P.P. Primary alanes and alanates: Useful synthetic reagents in aluminum chemistry. *Polyhedron* **2000**, *19*, 1649–1661. [CrossRef]
5. Aldridge, S.; Downs, A.J. Hydrides of Main-Group Metals: New Variations on an old theme. *Chem. Rev.* **2001**, *104*, 3305–3365. [CrossRef]
6. Orimo, S.; Nakamori, Y.; Eliseo, J.R.; Züttel, A.; Jensan, C.M. Complex Hydride for Hydrogen Storage. *Chem. Rev.* **2007**, *107*, 4111–4132. [CrossRef]
7. Graetz, J.; Reilly, J.J.; Yartys, V.A.; Maehlen, J.P.; Bulychev, B.M.; Antonov, V.E.; Tarasov, B.P.; Grabis, I.E. Aluminum hydride as a hydrogen and energy storage material: Past, present and future. *J. Alloy. Compd.* **2011**, *509*, S517–S528. [CrossRef]
8. Li, W.; Ma, X.; Walawalkar, M.G.; Yang, Z.; Roesky, H.W. Soluble aluminum hydrides function as catalysts in deprotonation, insertion, and activation reactions. *Coord. Chem. Rev.* **2017**, *350*, 14–29. [CrossRef]
9. Lansbury, P.T.; Peterson, J.O. Lithium *N*-Dihydroaluminum Hydride—A Selective Reducing Agent for Highly Electrophilic Carbonyl Compounds. *J. Am. Chem. Soc.* **1961**, *83*, 3537–3538. [CrossRef]
10. Lansbury, P.T.; Peterson, J.O. Novel Selectivity in Reduction of Ketones by Lithium *N*-Dihydroaluminum Hydride. *J. Am. Chem. Soc.* **1962**, *84*, 1756–1757. [CrossRef]
11. Lansbury, P.T.; Peterson, J.O. Lithium Tetrakis-(*N*-dihydropyridyl)-aluminate: Structure and Reducing Properties. *J. Am. Chem. Soc.* **1963**, *85*, 2236–2242. [CrossRef]
12. Tanner, D.D.; Yang, C.-M. On the Structure and Mechanism of Formation of the Lansbury Reagent, Lithium Tetrakis(*N*-dihydropyridyl)aluminate. *J. Org. Chem.* **1993**, *58*, 1840–1846. [CrossRef]
13. Hensen, K.; Lemke, A.; Stumpf, T.; Bolte, M.; Fleischer, H.; Pulham, C.R.; Gould, R.O.; Harris, S. Synthesis and Structural Characterization of (1,4-Dihydropyrid-1-yl)aluminum Complexes. *Inorg. Chem.* **1999**, *38*, 4700–4704. [CrossRef] [PubMed]
14. Less, R.J.; Simmonds, H.R.; Wright, D.S. Reactivity and catalytic activity of *tert*-butoxy-aluminium hydeide reagents. *Dalton Trans.* **2014**, *43*, 5785–5792. [CrossRef] [PubMed]
15. Stout, D.M.; Meyers, A.I. Recent Advances in the Chemistry of Dihydropyridines. *Chem. Rev.* **1982**, *82*, 223–243. [CrossRef]
16. Murosaki, T.; Kaneda, S.; Maruhashi, R.; Sadamori, K.; Shoji, Y.; Tamao, K.; Hashizume, D.; Hayakawa, N.; Matsuo, T. Synthesis and Structural Characteristics of Discrete Organoboron and Organoaluminum Hydirdes Incorporating Bulky Eind Groups. *Organometallics* **2016**, *35*, 3397. [CrossRef]
17. Nagata, K.; Murosaki, T.; Agou, T.; Sasamori, T.; Matsuo, T.; Tokitoh, N. Activation of Dihydrogen by Masked Doubly Bonded Aluminum Species. *Angew. Chem. Int. Ed.* **2016**, *55*, 12877–12880. [CrossRef] [PubMed]
18. Emsley, J. *The Elements*, 3rd ed.; Oxford University Press: Oxford, UK, 1998.
19. Matsuo, T.; Suzuki, K.; Fukawa, T.; Li, B.L.; Ito, M.; Shoji, Y.; Otani, T.; Li, L.C.; Kobayashi, M.; Hachiya, M.; et al. Synthesis and structures of a series of bulky "Rind-Br" based on a rigid fused-ring *s*-hydrindacene skeleton. *Bull. Chem. Soc. Jpn.* **2011**, *84*, 1178–1191. [CrossRef]
20. *CrysAlisPro*; Oxford Diffraction/Agilent Technologies UK Ltd.: Yarnton, UK, 2014.
21. *CrystalClear*; Rigaku/MSC. Inc.: The Woodlands, TX, USA, 2005.
22. Burla, M.C.; Caliandro, R.; Camalli, M.; Carrozzini, B.; Cascarano, G.L.; Giacovazzo, C.; Mallamo, M.; Mazzone, A.; Polidori, G.; Spagna, R. SIR2011. *J. Appl. Cryst.* **2012**, *45*, 357–361. [CrossRef]
23. Burla, M.C.; Caliandro, R.; Camalli, M.; Carrozzini, B.; Cascarano, G.L.; De Caro, L.; Giacovazzo, C.; Polidori, G.; Spagna, R. SIR2005. *J. Appl. Cryst.* **2005**, *38*, 381–388. [CrossRef]
24. Sheldrick, G.M. SHELXL-2018/3. *Acta Crystallogr. Sect. C* **2015**, *C71*, 3–8.